environmental microbiology reports

Environmental Microbiology Reports (2020) **12**(5), 555–567 doi:10.1111/1758-2229.12876

Brief Report

Substrate-dependent incorporation of carbon and hydrogen for lipid biosynthesis by *Methanosarcina barkeri*

Weichao Wu,[1†*] Travis B. Meador,[1,2,3] Martin Könneke,[1] Marcus Elvert,[1] Gunter Wegener[1,4] and Kai-Uwe Hinrichs[1]

[1]*Organic Geochemistry Group, MARUM-Centre for Marine Environmental Sciences and Department of Geosciences, University of Bremen, Bremen, 28359, Germany.*

[2]*Biology Centre Czech Academy of Sciences, Soil and Water Research Infrastructure, Ceske Budejovice, CZ-37005, Czechia.*

[3]*Faculty of Science, Department Ecosystem Biology, University of South Bohemia, Ceske Budejovice, CZ-37005, Czechia.*

[4]*Max Planck Institute for Marine Microbiology, Bremen, 28359, Germany.*

Summary

Dual stable isotope probing has been used to infer rates of microbial biomass production and modes of carbon fixation. In order to validate this approach for assessing archaeal production, the methanogenic archaeon *Methanosarcina barkeri* was grown either with H_2, acetate or methanol with D_2O and ^{13}C-dissolved inorganic carbon (DIC). Our results revealed unexpectedly low D incorporation into lipids, with the net fraction of water-derived hydrogen amounting to 0.357 ± 0.042, 0.226 ± 0.003 and 0.393 ± 0.029 for growth on H_2/CO_2, acetate and methanol respectively. The variability in net water H assimilation into lipids during the growth of *M. barkeri* on different substrates is possibly attributed to different Gibbs free energy yields, such that higher energy yield promoted the exchange of hydrogen between medium water and lipids. Because NADPH likely serves as the portal for H transfer, increased NADPH production and/or turnover associated with high energy yield may explain the apparent differences in net water H assimilation into lipids. The variable DIC and water H incorporation into *M. barkeri* lipids imply systematic, metabolic patterns of isotope incorporation and suggest that the ratio of ^{13}C-DIC versus D_2O assimilation in environmental samples may serve as a proxy for microbial energetics in addition to microbial production and carbon assimilation pathways.

Introduction

Stable isotopic compositions of microbial lipids provide valuable metabolic and taxonomic information that helps to decipher the role of microorganisms in biogeochemical cycles (Hayes, 1993; Hinrichs *et al*., 1999; Dawson *et al*., 2015). The $^{13}C/^{12}C$ ratio, expressed as $\delta^{13}C$, of microbial biomass is primarily determined by the carbon sources, fixation pathways and physiological conditions (e.g., Hinrichs *et al*., 1999; Hayes, 2001; Boschker and Middelburg, 2002; Schouten *et al*., 2004; Londry *et al*., 2008; Blaser *et al*., 2015), whereas the ratio of stable hydrogen isotopes (deuterium/protium ratio; D/H; expressed as δD) is determined by the water and substrate-based sources of hydrogen and the interactions of central metabolic pathways (Valentine, 2009; Zhang *et al*., 2009a; Wijker *et al*., 2019). The fractionation factors that determine the δD value of lipids versus source water vary systematically with specific metabolisms, showing a decrease in the order: heterotrophic growth on TCA-cycle precursors and intermediates > heterotrophic growth on sugars > photoautotrophy > chemoautotrophy (Valentine *et al*., 2004a; Sessions and Hayes, 2005; Zhang *et al*., 2009a).

Stable isotope probing (SIP) of diagnostic molecules (lipids or nucleic acids) with labelled substrates has been widely used because it can trace the activity of microbial communities and provide an estimate of key metabolic processes (Boschker *et al*., 1998; Kreuzer-Martin, 2007;

Received 15 March, 2019; accepted 7 August, 2020. *For correspondence. Tel. +46(0)86747245. E-mail wwcpku@gmail.com. †Present address: Biogeochemistry Group, Department of Environmental Science, Stockholm University, Stockholm 106 91, Sweden.

Taubert *et al*., 2018). Widely used ^{13}C-labelled substrates include dissolved inorganic carbon (DIC) and organic compounds such as glucose, amino acids and bulk biomass (Wegener *et al*., 2016). However, the utilization of organic substrates in SIP experiments distorts the *in situ* nutrition conditions, particularly for organic matter-lean microbial habitats, and it selects for a subpopulation of the microbial community, which probably characterizes a specific metabolic process rather than the entire community (Kopf *et al*., 2015).

Labeling experiments with heavy water (D_2O) have been an alternative to earlier established methods (e.g., ^{13}C and ^{15}N) to estimate total microbial biosynthesis activity (Wegener *et al*., 2012; Kopf *et al*., 2015; Wegener *et al*., 2016) and can even be used for sorting and identifying single active cells (Berry *et al*., 2015; Kopf *et al*., 2016; Taubert *et al*., 2018). Lipid-based SIP with D_2O provides a bulk, quantitative estimate of microbial community production, without altering natural conditions or selecting for certain autotrophic or heterotrophic C metabolisms, via the measurement of D incorporation into lipids via established gas chromatography-isotope ratio mass spectrometry. Water-derived hydrogen incorporation into lipids is essentially mediated by NADPH in the central metabolism (Zhang *et al*., 2009a; Berry *et al*., 2015; Wijker *et al*., 2019), where NADPH gains hydrogen from organic substrates or water-derived hydrogen via diverse metabolic processes such as glycolysis, the oxidative pentose phosphate pathway and the TCA cycle (Zhang *et al*., 2009a; Spaans *et al*., 2015; Wijker *et al*., 2019). Isotope labeling studies of fatty acid biosynthesis in heterotrophic bacteria indicate that NADPH is the most important H source (~50%) and controls the isotope effect during lipid biosynthesis, while the medium water (~25%) is of less importance relative to NADPH (Saito *et al*., 1980; Valentine, 2009; Zhang *et al*., 2009a; Osburn *et al*., 2016). In contrast, this is not true for archaea that derive their lipid hydrogen mainly from acetyl-CoA (~60%; Fig. S1, Jain *et al*., 2014; Rodriguez and Leyh, 2014; Vinokur *et al*., 2016). Despite this, the resulting δD values of lipids are generally well correlated with that of the medium water source (Valentine *et al*., 2004b; Zhang *et al*., 2009a; Zhang *et al*., 2009b; Dirghangi and Pagani, 2013a, 2013b), highlighting that water plays an additional indirect role (Zhang *et al*., 2009a) in determining lipid hydrogen isotopic composition by potential hydrogen exchange between NADPH and water. Due to the difficulty in determining the hydrogen isotopic composition of NADPH, two ultimate H sources (i.e., external water and organic substrates) are assumed to be incorporated into lipids, with the final lipid H isotopic composition determined by isotope effects of metabolic fluxes and the enzymes involved (Sessions and Hayes, 2005; Zhang *et al*., 2009a; Wijker *et al*., 2019). Therefore, the fractionation factor between water and lipids ($\alpha_{l/w}$) and the net water-derived hydrogen contribution (X_w) have to be considered for hydrogen assimilation during lipid biosynthesis (Sessions and Hayes, 2005; Zhang *et al*., 2009a; Kopf *et al*., 2015, 2016). In order to better understand this relationship, a physiological parameter 'water hydrogen assimilation constant (a_w)' was defined by Kopf *et al*. (2015), which was obtained from the regression of the hydrogen isotopic composition of lipids and water. Thus, a_w represents a net combination of the net hydrogen isotope fractionation factor and water hydrogen assimilation, and can indirectly provide the information of water-derived hydrogen for lipid biosynthesis (Sessions and Hayes, 2005; Zhang *et al*., 2009a; Kopf *et al*., 2015, 2016), which is relevant for the application of D_2O labeling in environmental studies. Reported a_w values of bacterial and eukaryotic fatty acids (Zhang and Sachs, 2007; Zhang *et al*., 2009a; Heinzelmann *et al*., 2015), alkenones (Englebrecht and Sachs, 2005; Schouten *et al*., 2006; van der Meer *et al*., 2015) and sterols (Sessions *et al*., 2002; Sachs and Schwab, 2011; Sachs and Kawka, 2015) in pure strain incubations and under different growth conditions range from 0.4 to 0.9 (Zhang and Sachs, 2007; Zhang *et al*., 2009a; Zhang *et al*., 2009b; Kopf *et al*., 2015, 2016). The parameter a_w is defined specifically for the application in isotope labeling work, and the diverse a_w values necessitate the use of a correction factor in order to accurately estimate microbial lipid production via the D_2O labeling approach (Kopf *et al*., 2015, 2016; Wegener *et al*., 2016).

Combined amendments with both ^{13}C-DIC and D_2O, also described as dual SIP, were developed to garner metabolic information without changing the *in situ* nutrient conditions (Kellermann *et al*., 2012, 2016; Wegener *et al*., 2012; Huguet *et al*., 2017). In these dual-SIP applications, the assumptions were: (i) independent of the carbon substrate utilized, most H incorporated into microbial lipids derives from water (>80%); (ii) assimilation of inorganic carbon (IC) into lipids of microbial heterotrophs is minor (<30%); and (iii) the ratio of ^{13}C (from IC) versus D (from water) incorporated into lipid biomarkers ($^{13}C\text{-}IC/D_2O_{assim}$) can distinguish the central microbial metabolism (~1 for autotrophs vs. <0.3 for heterotrophs). However, the diverse values of a_w imply the cut-off value for the distinction of the microbial metabolism could be variable. Similarly, an unconstrained contribution of IC during heterotrophic growth can complicate the use of $^{13}C\text{-}IC/D_2O_{assim}$ for isotope labeling experiments. These assumptions, based on experiments with the bacterium *Desulfosarcina variabilis* (Wegener *et al*., 2012), have not yet been validated for other microbes, especially for archaea.

Archaea play an important role in the biogeochemical carbon cycle in the ocean and in sediments (Könneke

et al., 2005; Thauer *et al*., 2008; Offre *et al*., 2013; Yu *et al*., 2018). In particular, methanogenic archaea, a widespread group of strictly anaerobic Euryarchaeota, can utilize diverse carbon substrates for energy metabolism like CO/CO_2 and H_2, formate, acetate and methanol or methylamines (Thauer *et al*., 2008), while methanotrophic archaea, on the other hand, turn over methane, which is represented by characteristic carbon isotopic compositions of archaeal lipids (Hinrichs *et al*., 1999; Elvert *et al*., 2000; Méhay *et al*., 2013; Zhuang *et al*., 2016). To our best knowledge, there is only one study on the a_w, investigating archaeol (AR) from a halophilic archaeon, *Haloarcula marismortui* (Dirghangi and Pagani, 2013b), but lipid a_w values of methanogens or other autotrophic archaea have rarely been constrained (Kaneko *et al.,* 2011; Könneke *et al.,* 2012). Thus, the correction factor of water hydrogen assimilation based on bacterial metabolisms might be not feasible when archaeal activity is studied using D_2O labelling. Moreover, if archaea also assimilate DIC when grown heterotrophically, as observed for the bacterium *Desulfosarcina variabilis* (cf. Wegener *et al*., 2012), it is necessary to investigate the contribution of DIC for archaeal lipid biosynthesis during heterotrophic growth. For methanogenic archaea, lipid biosynthesis is associated with an IC demand not only for autotrophic but also for heterotrophic growth, i.e., IC is fixed into the intermediate acetyl-CoA catalysed by the carbon monoxide dehydrogenase (CODH) enzyme, and further utilized for lipid biosynthesis (Thauer, 1998; Yin *et al*., 2019). However, it is not clear how much IC is flowing into lipid biosynthesis of methanogenic archaea during heterotrophic growth (Londry *et al*., 2008), and it thus hinders the dual SIP application and the elucidation of the carbon metabolic routes of methanogenic and, more generally, archaeal lipid biosynthesis in environmental samples.

In this study, we examined the methanogenic archaeon *Methanosarcina barkeri* cultured with diverse carbon substrates to better understand the mechanisms of carbon and hydrogen fixation into archaeal lipids using the dual SIP approach. Specifically, we (i) quantified the contribution of IC during lipid biosynthesis of *M. barkeri* grown under different substrate conditions (H_2/CO_2, acetate or methanol), (ii) followed the assimilation of water derived hydrogen into archaeal lipids produced under these conditions, and (iii) evaluated the ratios of ^{13}C-DIC and D_2O derived from carbon assimilation and lipid production rates respectively. Based on the acquired information, we were able to extend the utilization of the dual SIP approach to study the microbial activity of archaeal community members in natural settings.

Results

Metabolic activity and development of methane carbon isotopic composition

Methanol was completely consumed by *M. barkeri* within 4 days and methane was produced relatively rapidly, increasing to ~20% (v/v) of the headspace (Fig. 1A). Methane was produced more slowly when acetate or H_2/CO_2 were supplied as substrates (Fig. 1A). This indicates that *M. barkeri* grew most rapidly on methanol, followed by H_2/CO_2 and acetate, which is consistent with observations by Londry *et al*. (2008). More details about the incubation of *M. barkeri* are provided in the Supporting Information Experimental Procedures. The δ^{13}C values of CH_4 at the time of harvest varied with the different ^{13}C-labelled carbon substrates. When growing on acetate

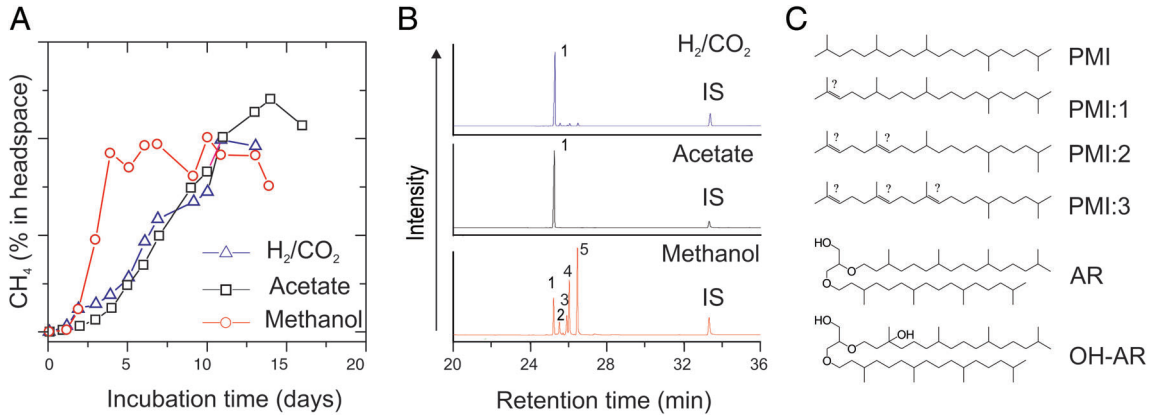

Fig 1. Production of CH_4 (v/v; %; A) in the headspace and relative concentrations of apolar lipids (B) in cultures of *M. barkeri* grown with the substrates H_2/CO_2, acetate and methanol (C) as well as structures of lipids in B. For B, peak 1 indicates 2,6,10,15,19-pentamethylicosane (PMI) and peaks 2–5 are pentamethylicosenes with 1–3 double bonds (unsPMIs). IS: the internal standard, squalane; AR, archaeol; OH-AR, hydroxyarchaeol.

and methanol with ^{13}C-bicarbonate the methane isotopic compositions were only moderately affected (Table S1). The δ^{13}C-CH_4 values of +38 to +215‰ suggest a minor contribution of IC to methane production for growth on the two organic substrates and are a result of back fluxes in the enzymatic chain of methanogenesis (Zehnder and Brock, 1979).

Substrate-dependent production of lipids

AR and hydroxyarchaeol (OH-AR) were the two dominant lipids of the polar lipid fraction in all experiments; the relative abundance of OH-AR (60%–70%) was higher than that for AR (30%–40%). Isoprenoid alkanes and alkenes were detected in the apolar fraction. Their distribution varied according to the carbon substrate. When grown on methanol, unsaturated pentamethylicosane derivatives (unsPMIs) with 1–3 double bonds accounted for 73%–96% (avg. 85%) of the total pentamethylicosanes (PMIs), whereas growth on H_2/CO_2 yielded only minor amounts of unsPMIs (<10%), and no unsPMIs were detected in incubations with acetate (Fig. 1B). This suggests the potential of unsPMIs as specific biomarker during the growth of *M. barkeri* on methanol.

Carbon isotopic composition of archaeal lipids during growth on specific substrates

When grown on unlabeled substrates, the net isotope fractionation between lipids and substrates varied substantially. For growth on acetate, lipids were enriched in ^{13}C relative to acetate with fractionation factor $\varepsilon_{lipid/acetate}$ of +0.85‰ to +3.62‰ (avg. +2.5‰; Supporting information Table S2). In contrast, lipids were depleted in ^{13}C with $\varepsilon_{lipid/substrate}$ of −24.6‰ and −21.1‰ for H_2/CO_2 and methanol respectively. Londry *et al*. (2008) also observed that lipids were enriched in ^{13}C on acetate but depleted on H_2/CO_2, however, the values of $\varepsilon_{lipid/substrate}$ were larger than in our study, e.g., $\varepsilon_{lipid/CO2}$ was up to −48.4‰ (Londry *et al*., 2008) versus −24.6‰ for growth on H_2/CO_2 in our study (Supporting information Table S2).

The incorporation of ^{13}C-labelled substrates with similar labeling strength during the growth on different energy substrates caused varying labeling intensity of the produced lipids. When grown on H_2/CO_2 with ^{13}C-bicarbonate, the δ^{13}C of lipids (+1590‰ to +2290‰) was slightly lower than the δ^{13}C values of total inorganic carbon (TIC) (δ^{13}C-TIC from +2410‰ to +2740‰). Based on the mass balance equation (Supporting Information Experimental Procedures), the contribution of TIC (X_{TIC}) in PMI, AR and OH-AR was 85.6 ± 8.5%, 87.8 ± 7.3% and 81.9 ± 11.9% respectively, with an average of X_{TIC} = 86.8 ± 7.4% (Fig. 2). If a kinetic isotope effect was considered (e.g., α = 1.052 for acetyl-CoA production from CO_2 by CODH; cf. Hayes, 2001), X_{TIC} would be more than 90%, suggesting that IC was the major carbon source for growth on H_2/CO_2, although the growth medium was supplemented with complex carbon substrates (e.g., yeast extracts and casitone).

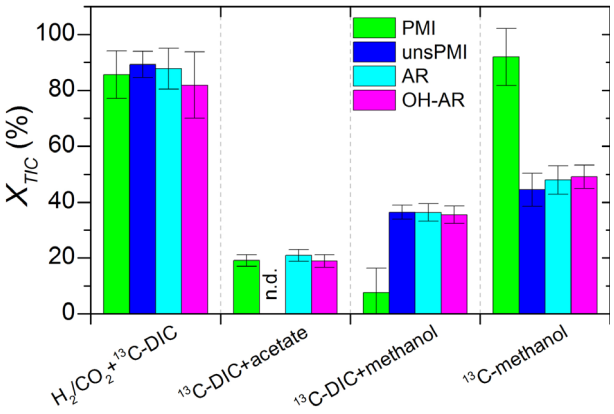

Fig 2. The molar fraction of *M. barkeri* lipid carbon derived from inorganic carbon (X_{TIC}; %) during growth on H_2/CO_2, acetate or methanol. Values determined by ^{13}C-substrate labeling according to Equations 1–3 in Supporting Information Experimental Procedures. n.d., not detected. X_{TIC} for lipids estimated from the 2-^{13}C-acetate experiment is not listed because X_{TIC} was not derived independently. Error bars are standard deviation from replicate samples (n = 3–5).

During growth of *M. barkeri* on acetate (δ^{13}C = −34.2‰) and labelled ^{13}C-bicarbonate (δ^{13}C- 3230‰ to 4370‰) lipids with δ^{13}C values of +670‰ to +730‰ were produced (Supporting information Table S1). This suggests that acetate was the major carbon source under these conditions. It was combined with minor utilization of smaller amounts of IC, and indeed X_{TIC} for the biosynthesis of PMI, AR and OH-AR was 19.1 ± 2.1%, 20.9 ± 2.1% and 18.9 ± 2.3% respectively (Fig. 2), with an average of 19.6 ± 2.2%. When *M. barkeri* was grown with 2-^{13}C-acetate (+1330‰ < δ^{13}C-acetate < +1830‰), the δ^{13}C values of PMI, AR and OH-AR were between +1540‰ and +2180‰ (for all data see Supporting information Table S1). The ^{13}C content of these lipids was higher than that of bulk acetate, suggesting that the methyl group of acetate is predominantly used for lipid synthesis. Based on mass balance equations (Equations 2 and 3 in Supporting Information Experimental Procedures), the contribution of methyl C (acetate-C2; X_{C2}) and carboxyl C (acetate-C1; X_{C1}) for lipid biosynthesis was on average 56.7 ± 1.7% and 23.7 ± 1.7% respectively (Fig. 2).

When grown on methanol with either ^{13}C-bicarbonate (+4250‰ < δ^{13}C-TIC< +8740‰) or ^{13}C-methanol (+4370‰ < δ^{13}C-methanol < +5560‰), the δ^{13}C values of unsPMIs, AR and OH-AR ranged from +1440‰ to +2960‰ (for all data see Supporting information Table S1) and were thus much lower than the label strength of IC or methanol. It

suggests that during growth on methanol *M. barkeri* uses both IC and methanol for the biosynthesis of its lipids. Based on the ^{13}C-bicarbonate experiment, X_{TIC} for the biosynthesis of unsPMIs, AR and OH-AR was 36.4 ± 2.6%, 36.3 ± 3.2%, 35.5 ± 3.3% respectively (Fig. 2), with an average of 36.2 ± 3.3%. By contrast, in the ^{13}C-methanol experiment, X_{TIC} for the biosynthesis of unsPMIs, AR and OH-AR was on average 46.2 ± 5.7% (Fig. 2). The difference could be due to the different isotopic fractionation effects between IC and lipids and methanol and lipids respectively, which were not considered in our calculation (cf. Equation 1 in Supporting Information Experimental Procedures). Notably, when ^{13}C-bicarbonate or ^{13}C-methanol was used, δ^{13}C-PMI was positive but always much lower (+7‰ to +1110‰; Supporting information Table S1) than that of other lipids, and even not related to the label strength of the carbon substrates. This led to an inconsistent estimate of X_{TIC} for PMI biosynthesis: the experiments with ^{13}C-bicarbonate yielded low values of X_{TIC} (7.6 ± 8.7%; Fig. 2) and those with ^{13}C-methanol yielded high values (92.0 ± 10.2%; Fig. 2). It indicates that unsPMIs were probably synthesized by *M. barkeri* during growth on methanol but PMI was not. unsPMIs, which are frequently observed in cold seep environments (Elvert *et al*., 1999, 2000; Pancost *et al*., 2001), might bear some potential as biomarker for the utilization of methanol or potentially other methylated substrates. Because neither bicarbonate nor methanol was apparent substrates for PMI synthesis during growth on methanol, the weighted average X_{TIC} for lipid biosynthesis (41.2 ± 6.7%) considered only the values determined for unsPMIs, AR and OH-AR via the two labeling strategies (i.e., ^{13}C-bicarbonate and ^{13}C-methanol).

Hydrogen isotopic composition of archaeal lipids during growth on various substrates

The δD of lipids varied with substrates when grown in unlabeled water medium (δD = −50.6‰) such that the hydrogen isotope fractionation factor between lipids and water was larger during growth on H_2/CO_2 ($\varepsilon_{lipid/water}$ = −279‰) compared with growth on acetate ($\varepsilon_{lipid/water}$ = −209‰) and methanol ($\varepsilon_{lipid/water}$ = −205‰; for all data see Supporting Information Table S3). Given that net fractionation factors of acetate and methanol are not as large as for H_2/CO_2, the fractionation factor between substrate and lipid could be larger than −200‰. This net isotope fractionation factor is an organism level fractionation factor that differs from the water hydrogen assimilation factor α_w (Equation 5 in Supporting Information Experimental Procedures). The varying fractionation factors for different substrates are consistent with the pattern that chemoautotrophy is generally associated with higher lipid-water hydrogen isotope fractionation than heterotrophy (Zhang *et al*., 2009a). This supports the notion that central metabolisms affect the archaeal lipid hydrogen isotope composition (Zhang *et al*., 2009a; Wijker *et al*., 2019).

During growth on deuterated medium (1% D_2O; equal to a δD of ~ + 64,000‰), the δD values of all three archaeal lipids ranged from +600 to +25 600‰ (Supporting information Table S1). Additional experiments with reduced label content (0.2% and 0.5% D_2O) yielded similar differences, indicating that this observation is not caused by an excessive labeling strength. This shows that lipid hydrogen of *M. barkeri* derives from multiple sources and not from water alone. Notably, for growth on methanol with a 1% D_2O treatment, δD-PMI was substantially lower and more variable (δD = +600 to +14,500‰) than that of unsPMIs, AR and OH-AR, suggesting that PMI was not primarily produced during growth on methanol, as also indicated by the ^{13}C labeling experiment.

In order to understand water-derived hydrogen contribution to lipid biosynthesis, a linear regression of the fractional D abundance (F^D) between water and lipids was applied (see Supporting information Experimental Procedures; Zhang *et al*., 2009a; Kopf *et al*., 2015; Kopf *et al*., 2016). During growth on H_2/CO_2, acetate or methanol, F^D of lipids correlated well with that of water in the medium (Fig. 3). The slope of regression was defined as the water hydrogen assimilation factor α_w, which represents the contribution of water hydrogen to lipid biosynthesis (Kopf *et al*., 2015, 2016). The average α_w for PMI, AR and OH-AR during the growth on H_2/CO_2 and acetate was 0.357 ± 0.042 and 0.226 ± 0.003 respectively (Fig. 3). However, when grown on methanol, the $F_{PMI}{}^D$ was not strongly correlated with water (R^2 = 0.35; Fig. 3) and α_w for PMI was lower (avg. 0.065 ± 0.065) than that for unsPMIs, AR and OH-AR (avg. 0.393 ± 0.029; Fig. 3). The large deviations of α_w for PMI are consistent with the questionable estimates of X_{TIC} for PMI during growth on methanol (see above).

Discussion

Substantial contribution of IC in lipid biosynthesis

IC fixation by methanogenic archaea is powered by H_2 consumption (electrons or protons) via the Wood–Ljungdahl pathway with CODH/acetyl-CoA synthetase (ACS) (Thauer, 1998; Ragsdale and Pierce, 2008). Our results demonstrate that IC is also an important C source (>20%) for lipid biosynthesis during heterotrophic growth on acetate and methanol. High IC requirement has also been observed in the lipid biosynthesis by methylotrophic methanogens (>60%; Yin *et al*., 2019) and by benthic archaeal communities in marine sediment incubations

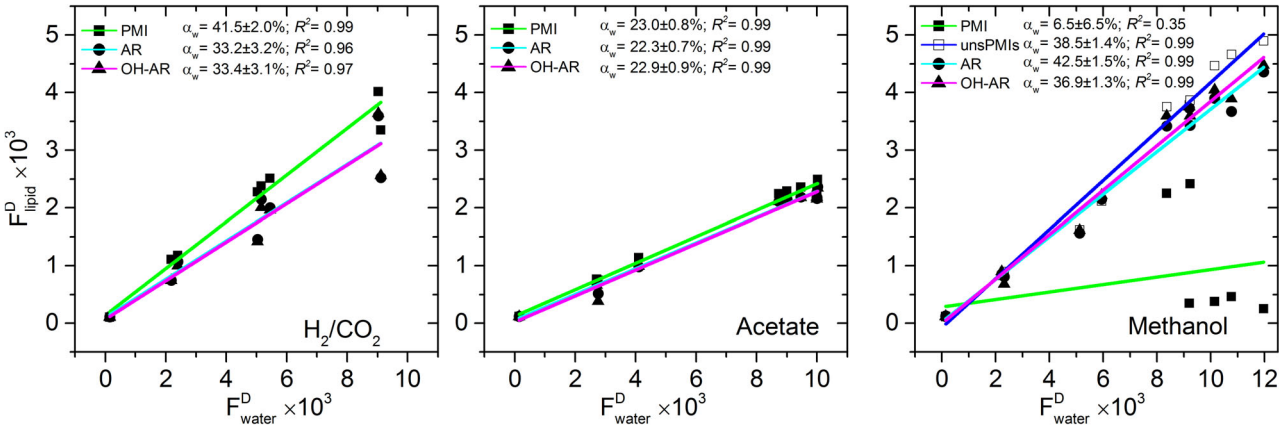

Fig 3. Relation of D fractional abundance ($F^D \times 10^3$) in lipids versus medium water for *M. barkeri* grown on H_2/CO_2, acetate or methanol. α_w is equal to the slope of the coefficients of the regression.

under methanogenic conditions (Evans *et al*., 2019), likely via the production of precursor acetyl-CoA for isoprenoid moieties of diether lipids (Fig. 4; Koga and Morii, 2005, 2007; Jain *et al*., 2014). During methanogenesis, the intermediate methyl-tetrahydromethanopterin (CH_3-H_4MPT) is converted to acetyl-CoA with the requirement of CO_2 by CODH/ACS enzymes (Fig. 4; Thauer, 1998), which is consistent with the high ^{13}C-labeling of acetate observed during growth on both (i) methanol in medium spiked with ^{13}C-methanol or ^{13}C-bicarbonate, and (ii) H_2/CO_2 in medium spiked with ^{13}C-bicarbonate (Supporting information Table S1). If the contribution of IC to acetate biosynthesis is calculated similarly as for lipids, we arrive at X_{TIC} values of 102 ± 6% and 48.5 ± 14.6% for growth on H_2/CO_2 and methanol respectively. During growth on methanol, roughly equivalent contributions of external IC

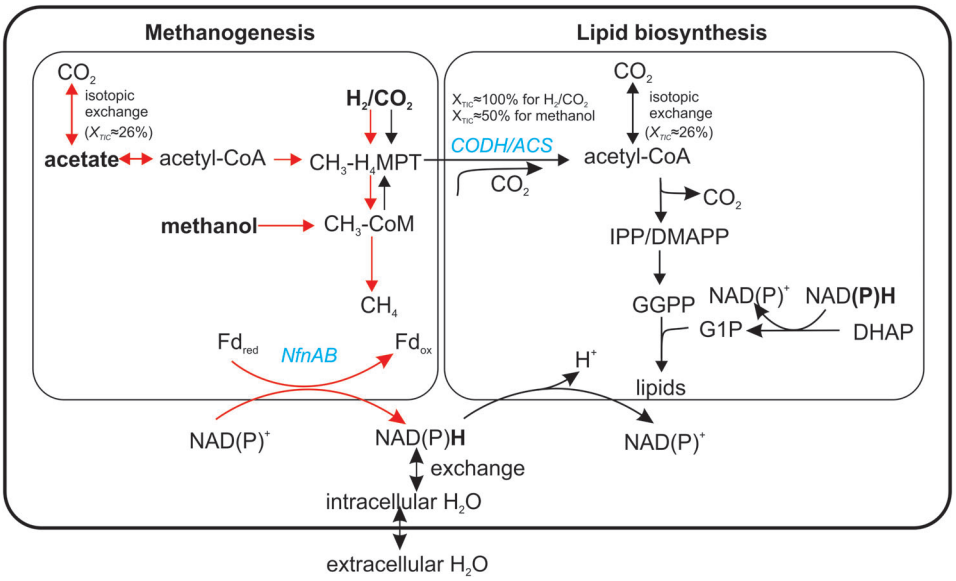

Fig 4. Schematic of methane production and lipid biosynthesis in methanogens (modified from Thauer, 1998; Koga and Morii, 2007; Londry *et al*., 2008; Jain *et al*., 2014). The black and red lines are lipid biosynthesis and methanogenesis pathways respectively. CH_3-H_4MPT, methyl-tetrahydromethanopterin; CH_3-CoM, methyl-coenzyme M; Fd_{ox}/Fd_{red}, oxidized and reduced ferredoxin; NADP/NADPH, nicotinamide adenine dinucleotide phosphate/reducing NADP; NAD/NADH, nicotinamide adenine dinucleotide/reducing NAD; IPP, isopentenyl pyrophosphate; DMAPP, dimethylallyl pyrophosphate; GGPP, geranylgeranyl pyrophosphate; G1P, *sn*-glycerol-1-phosphate; DHAP, dihydroxyacetone phosphate; CODH, carbon monoxide dehydrogenase; ACS, acetyl-CoA synthetase; NfnAB, NADH-dependent ferredoxin:NADP oxidoreductase. It notes that CO_2 in this figure refers to the contribution of total inorganic carbon (TIC). The carbon flow in the figure is explained as below: (i) $X_{TIC} \approx 100\%$ and 50% were the IC contributions for acetate biosynthesis for growth on H_2/CO_2 and methanol respectively, determined from the growth on H_2/CO_2 plus ^{13}C-DIC, and methanol plus ^{13}C-DIC or ^{13}C-methanol (cf. Equation 1 in Supporting Information Experimental Procedures). (ii) $X_{TIC} \approx 26\%$ is IC contribution to acetate-C1 due to isotopic exchange between $^{13}CO_2$ and acetate-C1, determined from the growth on acetate plus ^{13}C-DIC (cf. Equation 1 in Supporting Information Experimental Procedures).

and methanol to acetate synthesis are consistent with the notion that methanol and CO_2 form the methyl and carboxyl groups of acetate respectively (Kenealy and Zeikus, 1982; Fig. 4). Furthermore, ^{13}C-bicarbonate was incorporated into acetate during growth on methanol, indicating that *M. barkeri* utilized external IC for acetate production, even though CO_2 can be derived from methanol catabolically. In contrast, the contribution of IC to lipid biosynthesis (X_{TIC} = 86.8 ± 7.4%) was less than that for acetate production during growth on H_2/CO_2, suggesting that organic substrates (e.g., yeast extract, casitone and cysteine) were essential components of the growth medium that contribute to lipid biosynthesis, e.g., the glycerol backbone of lipids, which accounts for 3 C atoms in AR and thus roughly 7% of lipid C. The contribution of IC to lipids during growth on methanol (X_{TIC} = 36.2 ± 3.3%) was also less than that for acetate production, implying ^{13}C-label dilution and/or loss of IC during the condensation of acetyl-CoA to isoprenoid moieties (Fig. S1).

Because acetate can be directly converted to acetyl-CoA by acetate kinase and phosphotransacetylase during acetoclastic methanogenesis (Fig. 4), it seems that IC is not required to form acetyl-CoA. However, the incorporation of ^{13}C-bicarbonate into lipids during growth on acetate suggests that IC may be assimilated via 'isotopic exchange' between CO_2 and the carbonyl moiety of acetyl-CoA (Eikmanns and Thauer, 1984), which is supported by the observation of ^{13}C enriched acetate at harvest for the treatment with ^{13}C-bicarbonate and natural acetate (Supporting information Table S1). No carbon exchange between other one-carbon substrates (e.g., formate and CO) and acetate was observed by methanogens (Eikmanns and Thauer, 1984), suggesting that this exchange requires electrochemical proton potential (Laufer *et al*., 1987). Another possibility is that the biosynthesis of acetyl-CoA actually included the disassembly and reassembly of acetyl-CoA for the further transfer of methyl group catalysed by nickel-containing CODH enzymes (Ragsdale and Wood, 1985; Ragsdale and Pierce, 2008). Therefore, this isotopic exchange mechanism may serve as a portal of IC assimilation in acetoclastic methanogenesis. A simple mass balance (e.g., Equation 1 in Supporting information Experimental Procedures) based on the ^{13}C enrichment of acetate (Supporting information Table S1) suggests that 26.1 ± 2.8% of acetate C was derived from IC by the end of the growth phase. The lower X_{TIC} value for lipid biosynthesis (19.6 ± 2.2%) relative to that for acetate production may result from the loss of CO_2 via cleavage of carboxylic group of acetate during lipid biosynthesis via the mevalonate (MVA) pathway (Supporting information Fig. S1). This is also implied from the varying contribution of acetate-C1 (carboxylic carbon; 23.7 ± 1.7%) and acetate-C2 (methyl carbon; 56.7 ± 1.7%) to lipids. The higher degree of incorporation of acetate-C2 suggests that these lipids were predominantly synthesized via the classic MVA pathway, where acetate-C2 and acetate-C1 are incorporated via acetyl-CoA into the five-carbon isoprenoid unit at a ratio of 1.5 (Koga and Morii, 2007). The much higher ratio 2.4 of acetate-C2 to C1 suggested by our findings implies relatively higher decarboxylation of acetate-C1 during the biosynthesis of GGPP from acetyl-CoA (Fig. 4; Supporting information Fig. S1). Preferential incorporation of acetate-C2 into membrane lipids is consistent with previous investigations of *Methanospirillum hungatei* (Ekiel *et al*., 1983) and *Sulfolobus solfataricus* (Rosa and Gambacorta, 1986).

Constraints of water-derived hydrogen to lipid biosynthesis

The relatively low water-derived hydrogen contribution observed in *M. barkeri* (<40%, Fig. 3) compared with acetogens (59%; Valentine *et al*., 2004a) or bacteria (>40%; Zhang *et al*., 2009a) suggests that the majority of lipid hydrogen was derived from the substrate (i.e., H_2, acetate and/or methanol). For hydrogenotrophic methanogenesis, we expect the molar hydrogen contribution of water to lipids (X_w; Equation 4 in Supporting Information Experimental Procedures) to be 100% if there was a very rapid hydrogen exchange between H_2 and HDO (Valentine *et al*., 2004a). For hydrogenotrophic *M. barkeri*, the overall hydrogen isotope fractionation ($\varepsilon_{l/w}$ = (1 - a_w) × 1000‰) between lipid and water determined in the current study for PMI, AR and OH-AR ranged from −669 to −627‰. It suggests that a large fractionation effect could play an important role for water hydrogen assimilation during hydrogenotrophic growth. The isotope effect for D incorporation into archaeal lipids is substantially larger than observed for growth on H_2/CO_2 by the acetogenic bacterium *Sporomusa* sp. ($\varepsilon_{l/w}$ = −410‰; Valentine *et al*., 2004a) as well as other bacteria (Zhang *et al*., 2009a). First, H_2 could be directly incorporated into intermediate methylene-H_4MPT via the reduction from H_2 to F420-H_2 by the coenzyme F420 (Thauer *et al*., 2008). Furthermore, methylene-H_4MPT is converted to acetyl-CoA. Thus, H_2 gas could partially contribute to lipid H. Although acetogenic bacteria and methanogenic archaea use the same pathway to fix H_2/CO_2 (i.e., Wood-Ljungdahl pathway; Ragsdale and Pierce, 2008), the higher hydrogenase efficiency (or molecular H_2 utilization efficiency) by methanogenic archaea (~50%; Valentine *et al*., 2004b) relative to acetogenic bacteria (<20%; Valentine *et al*., 2004a) may indicate less time for isotope exchange between H_2 and HDO and more H_2 molecular contribution into lipid by *M. barkeri*. The relatively low a_w of *M. barkeri* growing on H_2/CO_2 may therefore be

achieved by the rapid assimilation of H_2 and thus less time and larger isotopic fractionation during H_2/HDO equilibration.

During acetoclastic and methylotrophic methanogenesis, *M. barkeri* appears to rather lower the water-derived hydrogen contribution by incorporating hydrogen from the methyl groups of acetate and methanol into lipids (Fig. 5; Supporting Information Fig. S1). We estimate that high portions of hydrogen are contributed through the substrate via the C skeleton of acetyl-CoA (50 of 88 hydrogen atoms in AR, ~57%) and NADPH (30 of 88 hydrogen atoms in AR, ~34%) may be assimilated into archaeal lipids (Supporting Information Fig. S1; Jain *et al*., 2014; Rodriguez and Leyh, 2014; Vinokur *et al*., 2016), with the remainder deriving from the water via the reduction of double bonds catalysed by geranylgeranyl diphosphate reductase (about 9%; 8 of 88 hydrogen atoms, Supporting Information Fig. S1). This contrasts the relative contribution of hydrogen sources to bacterial fatty acid biosynthesis (50%, 25%, and 25% for NADPH, substrate, and water respectively; Valentine, 2009; Zhang *et al*., 2009a; Wijker *et al*., 2019). The relatively high contribution of hydrogen atoms derived from sources other than water to archaeal methanogen lipids is consistent with >50% of lipid C being derived from the ^{13}C-labelled methyl groups of methanol or acetate (see Results). Therefore, the incorporation of water-derived hydrogen into the archaeal methanogen cell membrane is likely buffered by the contribution of substrate methyl group-derived hydrogen to the acetyl-CoA precursor of the MVA pathway, yielding relatively low a_w values compared with other microbes (e.g., Valentine *et al*., 2004a; Zhang *et al*., 2009a). However, this mechanism alone cannot explain the difference in a_w between acetoclastic versus methylotrophic methanogenesis as well as net hydrogen isotope fractionation between lipid and water (Fig. 3), unless the isotope fractionation of metabolic water and its contribution to transhydrogenation reactions in the MVA pathway are completely opposite for the two metabolisms (Fig. 4 and Fig. S1). A more likely driver of the observed isotope effects is the process of NADPH-mediated exchange of hydrogen ions between water and lipids (Valentine, 2009; Zhang *et al*., 2009a; Wijker *et al*., 2019; Supporting Information Fig. S1).

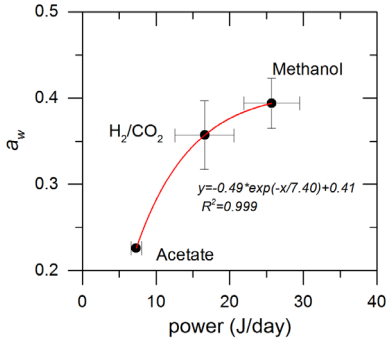

Fig 5. Relationship of power derived from methanogenesis (J day^{-1}) and water hydrogen assimilation factor a_w. The power supply is calculated by multiplying the methane production rate (mmol CH_4 day^{-1}) by Gibbs free energy potential (kJ mol^{-1} CH_4) under initial conditions (details see Supporting Information Table S5 and Text S1).

Archaeal methanogens can metabolize substrates to acetyl-CoA via pathways that do not produce NADPH (Weimer and Zeikus, 1978; Fig. 4). Genome analysis suggests that *M. barkeri* and other methanogens are unlikely to generate NADPH similarly to bacteria, who gain energy via glycolysis, the oxidative pentose phosphate pathway, and/or the TCA cycle (Allen *et al*., 2009; Zhang *et al*., 2009a; Sakai *et al*., 2011; Spaans *et al*., 2015). Instead, the exergonic reduction of $NADP^+$ to NADPH coupled with ferredoxin by transhydrogenase NADH-dependent ferredoxin:NADP oxidoreductase (NfnAB) is likely the main NADPH production pathway for archaea (Huang *et al*., 2012; Spaans *et al*., 2015). Ferredoxin is widespread among methanogens containing cytochromes (e.g., *Methanosarcina* species) and additionally plays an important role in methane production (Thauer *et al*., 2008). NfnAB is thus coupled to microbial energy conservation (Buckel and Thauer, 2013; Spaans *et al*., 2015) and is hypothesized to have a significant effect on the hydrogen isotopic compositions of lipids from anaerobic bacteria (e.g., sulfate-reducing bacteria; Leavitt *et al*., 2016; Osburn *et al*., 2016). Accordingly, NADPH generated via NfnAB can exchange hydrogen ions with intercellular water (Fig. 4), thereby introducing both kinetic and equilibrium isotope effects. A fast turnover of NADPH presumably results in a kinetic isotope effect, while low turnover in an equilibrium isotope effect. As such, modulations of NADPH pool size, turnover time, and D/H isotopic composition may therefore explain the observed relationship between $a_{l/w}$ exhibited by *M. barkeri* and energy supply (or power requirement expressed in J/day; Hoehler and Jørgensen, 2013; LaRowe and Amend, 2015; Lever *et al*., 2015; Fig. 5).

A mass balance of hydrogen sources of lipids in *M. barkeri* (adopted from Wijker *et al*., 2019) indicates that the combined hydrogen isotope effects of NADPH production ($\varepsilon_{NADPH/w}$) during acetoclastic versus methylotrophic methanogenesis are offset by approximately 300‰ and may be as large as -635 ± 60 and -305 ± 155‰ respectively (Supporting Information Text). The relationship between a_w and energy demand could result from either a decreasing residual pool of NADPH for lipid biosynthesis during rapid growth on methanol, which would yield smaller $\varepsilon_{NADPH/w}$ via Rayleigh fractionation, or an increased amount of time for NADPH to equilibrate with HDO. These findings are consistent with those by Penning *et al*. (2005), who demonstrated that

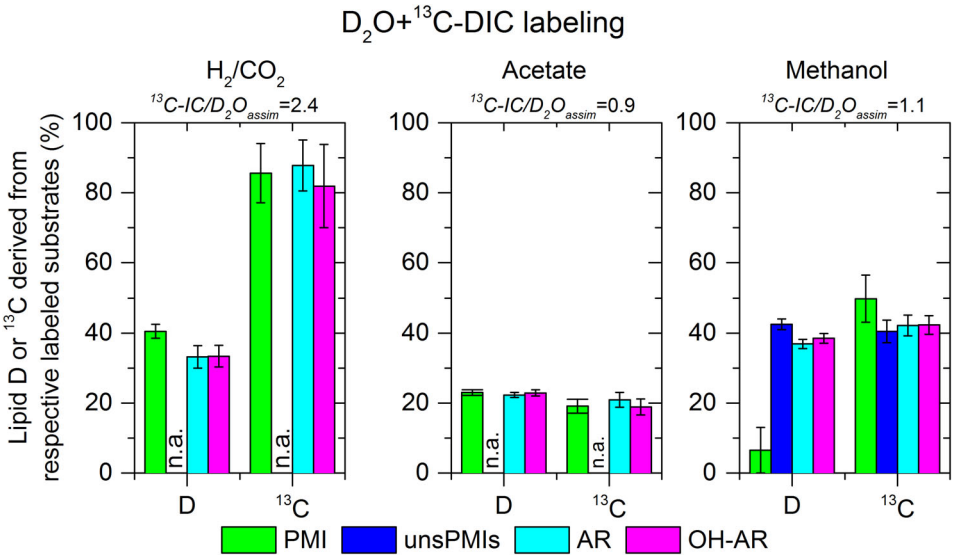

Fig 6. Incorporation ratio of ^{13}C-DIC and D_2O into characteristic lipids ($^{13}C\text{-}IC/D_2O_{assim}$) produced by *M. barkeri* grown on different substrates. $^{13}C\text{-}IC/D_2O_{assim}$ values are noted above the figure and represent the average for all lipids. Due to the disparity of PMI for growth on methanol, $^{13}C\text{-}IC/D_2O_{assim}$ was determined from the average of unsPMIs, AR and OH-AR. n.a., not applicable.

the carbon isotopic fractionation of methane produced by methanogenic cultures was controlled by the Gibbs free energy change of methane formation and potentially also by the intracellular availability of CO_2 (Valentine et al.,2004b). In summary, our parallel C and H isotope data for hydrogenotrophic, acetoclastic and methylotrophic methanogenesis suggest that ferredoxin-regulated hydrogen exchange between extracellular water and intracellular NADPH may ultimately determine the assimilation of hydrogen into membrane lipids.

Implication for the dual SIP approach

Using dual SIP with D_2O and ^{13}C-DIC, the ratio of ^{13}C versus D incorporation into lipids ($^{13}C\text{-}IC/D_2O_{assim}$) can distinguish autotrophic versus heterotrophic modes of carbon assimilation (cf. Wegener *et al*., 2012). Based on experiments utilizing the sulfate-reducing bacterium *D. variabilis*, $^{13}C\text{-}IC/D_2O_{assim}$ values were identified to be 1 and 0.3 during autotrophic and heterotrophic growth respectively (Wegener *et al*., 2012) and thus an $^{13}C\text{-}IC/D_2O_{assim}$ value of 0.3 was set as a 'cut-off' value to estimate the contribution of heterotrophic IC fixation. In contrast to experiments by Wegener *et al*. (2012), *M. barkeri* exhibited a very different pattern of ^{13}C and D incorporation with values for $^{13}C\text{-}IC/D_2O_{assim}$ of 2.4, 0.9 and 1.1 for growth on H_2/CO_2, acetate and methanol respectively (Fig. 6), owing to the relatively lower contribution of water-derived hydrogen to lipid biosynthesis. In order to account for the incorporation of hydrogen from sources other than water into membrane lipids, such as acetyl-CoA, we applied an a_w correction factor of 0.33, based on the average of all three growth conditions. Accordingly, $^{13}C\text{-}IC/D_2O_{assim}$ values were reduced to 0.78, 0.28 and 0.30 for growth on H_2/CO_2, acetate and methanol respectively. This indicates that future estimates of archaeal lipid production based on D incorporation should consider the water hydrogen assimilation factor (a_w) (Kopf *et al*., 2016; Wegener *et al*., 2016) to distinguish between archaeal auto- and hetero-trophy. We suggest a correction factor a_w of 0.67 (Wegener *et al*., 2012) and 0.33 (this study) to be used while estimating bacterial and methanogenic archaeal lipid production in marine environmental samples respectively. In conclusion, the application of dual SIP employing D_2O and ^{13}C-DIC should consider variations of water-derived hydrogen discrimination caused by different microorganisms as wells as carbon substrates, which complicates the use of $^{13}C\text{-}IC/D_2O_{assim}$ as a proxy estimating the contribution of heterotrophic versus autotrophic lipid sources.

Acknowledgements

This work was primarily funded by the Deutsche Forschungsgemeinschaft through the Gottfried Wilhelm Leibniz Price to KUH (HI 616-14/1), which included the purchase of the isotope ratio infrared spectrometer used in this study as well as partial support of W.W., T.B.M., and M.K. W. Wu was primarily funded by a scholarship from the China Scholarship Council (CSC). T.B.M. was additionally supported by MEYS CZ grant LM2015075 Projects of Large Infrastructure for Research, Development and Innovations as well as the European Regional Development Fund-Project: Research of key soil–water ecosystem interaction at the SoWa Research Infrastructure (No. CZ.02.1.01/0.0/0.0/16_013/0001782). We

thank X. P. Mollar, J. Wendt, H. Taubner, E. Schefuß and M. Kölling at MARUM for their support for $\delta^{13}C$ and δD measurements. We also thank M. Lever in the Department of Environmental System Sciences at Swiss Federal Institute of Technology Zurich, Switzerland, for Gibbs energy calculation. We are very grateful to Sebastian Kopf and an anonymous reviewer for their constructive comments and stimulating suggestions that substantially improved the manuscript.

References

Allen, M.A., Lauro, F.M., Williams, T.J., Burg, D., Siddiqui, K. S., De Francisci, D., *et al*. (2009) The genome sequence of the psychrophilic archaeon, *Methanococcoides burtonii*: the role of genome evolution in cold adaptation. *ISME J* **3**: 1012–1035.

Berry, D., Mader, E., Lee, T.K., Woebken, D., Wang, Y., Zhu, D., *et al*. (2015) Tracking heavy water (D_2O) incorporation for identifying and sorting active microbial cells. *Proc Natl Acad Sci U S A* **112**: E194–E203.

Blaser, M.B., Dreisbach, L.K., and Conrad, R. (2015) Carbon isotope fractionation of *Thermoanaerobacter kivui* in different growth media and at different total inorganic carbon concentration. *Org Geochem* **81**: 45–52.

Boschker, H.T.S., and Middelburg, J.J. (2002) Stable isotopes and biomarkers in microbial ecology. *FEMS Microbiol Ecol* **40**: 85–95.

Boschker, H.T.S., Nold, S.C., Wellsbury, P., Bos, D., der Graaf, W., Pel, R., *et al*. (1998) Direct linking of microbial populations to specific biogeochemical processess by ^{13}C-labelling of biomarkers. *Nature* **392**: 801–805.

Buckel, W., and Thauer, R.K. (2013) Energy conservation via electron bifurcating ferredoxin reduction and proton/Na^+ translocating ferredoxin oxidation. *Biochim Biophys Acta Bioenergetics* **1827**: 94–113.

Dawson, K.S., Osburn, M.R., Sessions, A.L., and Orphan, V. J. (2015) Metabolic associations with archaea drive shifts in hydrogen isotope fractionation in sulfate-reducing bacterial lipids in cocultures and methane seeps. *Geobiology* **13**: 462–477.

Dirghangi, S.S., and Pagani, M. (2013a) Hydrogen isotope fractionation during lipid biosynthesis by *Tetrahymena thermophila*. *Org Geochem* **64**: 105–111.

Dirghangi, S.S., and Pagani, M. (2013b) Hydrogen isotope fractionation during lipid biosynthesis by *Haloarcula marismortui*. *Geochim Cosmochim Acta* **119**: 381–390.

Eikmanns, B., and Thauer, R. (1984) Catalysis of an isotopic exchange between CO_2 and the carboxyl group of acetate by *Methanosarcina barkeri* grown on acetate. *Arch Microbiol* **138**: 365–370.

Ekiel, I., Smith, I., and Sprott, G.D. (1983) Biosynthetic pathways in Methanospirillum hungatei as determined by ^{13}C nuclear magnetic resonance. *J Bacteriol* **156**: 316–326.

Elvert, M., Suess, E., Greinert, J., and Whiticar, M.J. (2000) Archaea mediating anaerobic methane oxidation in deep-sea sediments at cold seeps of the eastern Aleutian subduction zone. *Org Geochem* **31**: 1175–1187.

Elvert, M., Suess, E., and Whiticar, M.J. (1999) Anaerobic methane oxidation associated with marine gas hydrates: superlight C-isotopes from saturated and unsaturated C_{20} and C_{25} irregular isoprenoids. *Naturwissenschaften* **86**: 295–300.

Englebrecht, A.C., and Sachs, J.P. (2005) Determination of sediment provenance at drift sites using hydrogen isotopes and unsaturation ratios in alkenones. *Geochim Cosmochim Acta* **69**: 4253–4265.

Evans T.W., Coffinet S., Könneke M., Lipp J.S., Becker K. W., Elvert M., Heuer V., Hinrichs K-U. (2019). Assessing the carbon assimilation and production of benthic archaeal lipid biomarkers using lipid-RIP. *Geochimica et Cosmochimica Acta*, **265**: 431–442. http://dx.doi.org/10.1016/j.gca.2019.08.030.

Hayes, J.M. (1993) Factors controlling ^{13}C contents of sedimentary organic compounds: principles and evidence. *Mar Geol* **113**: 111–125.

Hayes, J.M. (2001) Fractionation of carbon and hydrogen isotopes in biosynthetic processes. *Rev Mineral Geochem* **43**: 225–277.

Heinzelmann, S.M., Villanueva, L., Sinke-Schoen, D., Damsté, J.S.S., Schouten, S., and Van der Meer, M.T. (2015) Impact of metabolism and growth phase on the hydrogen isotopic composition of microbial fatty acids. *Front Microbiol* **6**: 408.

Hinrichs, K.U., Hayes, J.M., Sylva, S.P., Brewer, P.G., and Delong, E.F. (1999) Methane-consuming archaebacteria in marine sediment. *Science* **398**: 802–805.

Hoehler, T.M., and Jørgensen, B.B. (2013) Microbial life under extreme energy limitation. *Nat Rev Microbiol* **11**: 83–94.

Huang, H., Wang, S., Moll, J., and Thauer, R.K. (2012) Electron bifurcation involved in the energy metabolism of the acetogenic bacterium *Moorella thermoacetica* growing on glucose or H_2 plus CO_2. *J Bacteriol* **194**: 3689–3699.

Huguet, A., Meador, T.B., Laggoun-Défarge, F., Könneke, M., Wu, W., Derenne, S., and Hinrichs, K.-U. (2017) Production rates of bacterial tetraether lipids and fatty acids in peatland under varying oxygen concentrations. *Geochim Cosmochim Acta* **203**: 103–116.

Jain, S., Caforio, A., and Driessen, A.J.M. (2014) Biosynthesis of archaeal membrane ether lipids. *Front Microbiol* **5**: 641.

Kaneko, M., Kitajima, F., and Naraoka, H. (2011) Stable hydrogen isotope measurement of archaeal ether-bound hydrocarbons. *Org Geochem* **42**: 166–172.

Kellermann, M.Y., Wegener, G., Elvert, M., Yoshinaga, M.Y., Lin, Y.S., Holler, T., *et al*. (2012) Autotrophy as a predominant mode of carbon fixation in anaerobic methane-oxidizing microbial communities. *Proc Natl Acad Sci U S A* **109**: 19321–19326.

Kellermann, M.Y., Yoshinaga, M.Y., Wegener, G., Krukenberg, V., and Hinrichs, K.-U. (2016) Tracing the production and fate of individual archaeal intact polar lipids using stable isotope probing. *Org Geochem* **95**: 13–20.

Kenealy, W.R., and Zeikus, J.G. (1982) One-carbon metabolism in methanogens: evidence for synthesis of a two-carbon cellular intermediate and unification of catabolism and anabolism in *Methanosarcina barkeri*. *J Bacteriol* **151**: 932–941.

Koga, Y., and Morii, H. (2005) Recent advances in structural research on ether lipids from archaea including

comparative and physiological aspects. *Biosci Biotechnol Biochem* **69**: 2019–2034.

Koga, Y., and Morii, H. (2007) Biosynthesis of ether-type polar lipids in archaea and evolutionary considerations. *Microbiol Mol Biol Rev* **71**: 97–120.

Könneke, M., Bernhard, A.E., de la Torre, J.R., Walker, C.B., Waterbury, J.B., and Stahl, D.A. (2005) Isolation of an autotrophic ammonia-oxidizing marine archaeon. *Nature* **437**: 543–546.

Könneke, M., Lipp, J.S., and Hinrichs, K.-U. (2012) Carbon isotope fractionation by the marine ammonia-oxidizing archaeon Nitrosopumilus maritimus. *Org Geochem* **48**: 21–24.

Kopf, S.H., McGlynn, S.E., Green-Saxena, A., Guan, Y., Newman, D.K., and Orphan, V.J. (2015) Heavy water and ^{15}N labeling with NanoSIMS analysis reveals growth-rate dependent metabolic heterogeneity in chemostats. *Environ Microbiol* **17**: 2542–2556.

Kopf, S.H., Sessions, A.L., Cowley, E.S., Reyes, C., Van Sambeek, L., Hu, Y., *et al*. (2016) Trace incorporation of heavy water reveals slow and heterogeneous pathogen growth rates in cystic fibrosis sputum. *Proc Natl Acad Sci U S A* **113**: E110–E116.

Kreuzer-Martin, H.W. (2007) Stable isotope probing: linking functional activity to specific members of microbial communities. *Soil Sci Soc Am J* **71**: 611–619.

LaRowe, D.E., and Amend, J.P. (2015) Power limits for microbial life. *Front Microbiol* **6**: 718.

Laufer K., Eikmanns B., Frimmer U., Thauer R.K (1987). Methanogenesis from Acetate by Methanosarcina barkeri: Catalysis of Acetate Formation from Methyl Iodide, CO2 , and H2 by the Enzyme System Involved. *Zeitschrift für Naturforschung C*, **42**: 360–372. http://dx.doi.org/10.1515/znc-1987-0407.

Leavitt, W.D., Flynn, T.M., Suess, M.K., and Bradley, A.S. (2016) Transhydrogenase and growth substrate influence lipid hydrogen isotope ratios in *Desulfovibrio alaskensis* G20. *Front Microbiol* **7**: 918.

Lever, M.A., Rogers, K.L., Lloyd, K.G., Overmann, J., Schink, B., Thauer, R.K., *et al*. (2015) Life under extreme energy limitation: a synthesis of laboratory- and field-based investigations. *FEMS Microbiol Rev* **39**: 688–728.

Londry, K.L., Dawson, K.G., Grover, H.D., Summons, R.E., and Bradley, A.S. (2008) Stable carbon isotope fractionation between substrates and products of *Methanosarcina barkeri*. *Org Geochem* **39**: 608–621.

Méhay, S., Früh-Green, G.L., Lang, S.Q., Bernasconi, S.M., Brazelton, W.J., Schrenk, M.O., *et al*. (2013) Record of archaeal activity at the serpentinite-hosted lost City hydrothermal field. *Geobiology* **11**: 570–592.

Offre, P., Spang, A., and Schleper, C. (2013) Archaea in biogeochemical cycles. *Annu Rev Microbiol* **67**: 437–457.

Osburn, M.R., Dawson, K.S., Fogel, M.L., and Sessions, A. L. (2016) Fractionation of hydrogen isotopes by sulfate- and nitrate-reducing bacteria. *Front Microbiol* **7**: 1166.

Pancost, R.D., Hopmans, E.C., and Sinninghe Damsté, J.S. (2001) Archaeal lipids in Mediterranean cold seeps: molecular proxies for anaerobic methane oxidation. *Geochim Cosmochim Acta* **65**: 1611–1627.

Penning, H., Plugge, C.M., Galand, P.E., and Conrad, R. (2005) Variation of carbon isotope fractionation in hydrogenotrophic methanogenic microbial cultures and environmental samples at different energy status. *Glob Chang Biol* **11**: 2103–2113.

Ragsdale, S.W., and Pierce, E. (2008) Acetogenesis and the Wood–Ljungdahl pathway of CO_2 fixation. *Biochim Biophys Acta* **1784**: 1873–1898.

Ragsdale, S.W., and Wood, H.G. (1985) Acetate biosynthesis by acetogenic bacteria. Evidence that carbon monoxide dehydrogenase is the condensing enzyme that catalyzes the final steps of the synthesis. *J Biol Chem* **260**: 3970–3977.

Rodriguez, S.B., and Leyh, T.S. (2014) An enzymatic platform for the synthesis of isoprenoid precursors. *PLoS One* **9**: e105594.

Rosa, M.D., and Gambacorta, A. (1986) Lipid biogenesis in archaebacteria. *Syst Appl Microbiol* **7**: 278–285.

Sachs, J.P., and Kawka, O.E. (2015) The influence of growth rate on $^{2}H/^{1}H$ fractionation in continuous cultures of the coccolithophorid *Emiliania huxleyi* and the diatom *Thalassiosira pseudonana*. *PLoS One* **10**: e0141643.

Sachs, J.P., and Schwab, V.F. (2011) Hydrogen isotopes in dinosterol from the Chesapeake Bay estuary. *Geochim Cosmochim Acta* **75**: 444–459.

Saito, K., Kawaguchi, A., Okuda, S., Seyama, Y., and Yamakawa, T. (1980) Incorporation of hydrogen atoms from deuterated water and stereospecifically deuterium-labeled nicotinamide nucleotides into fatty acids with the *Escherichia coli* fatty acid synthetase system. *Biochim Biophys Acta* **618**: 202–213.

Sakai, S., Takaki, Y., Shimamura, S., Sekine, M., Tajima, T., Kosugi, H., *et al*. (2011) Genome sequence of a mesophilic hydrogenotrophic *Methanogen Methanocella paludicola*, the first cultivated representative of the order *Methanocellales*. *PLoS One* **6**: e22898.

Schouten, S., Ossebaar, J., Schreiber, K., Kienhuis, M.V.M., Langer, G., Benthien, A., and Bijma, J. (2006) The effect of temperature, salinity and growth rate on the stable hydrogen isotopic composition of long chain alkenones produced by *Emiliania huxleyi* and *Gephyrocapsa oceanica*. *Biogeosciences* **3**: 113–119.

Schouten, S., Strous, M., Kuypers, M.M., Rijpstra, W.I.C., Baas, M., Schubert, C.J., *et al*. (2004) Stable carbon isotopic fractionations associated with inorganic carbon fixation by anaerobic ammonium-oxidizing bacteria. *Appl Environ Microbiol* **70**: 3785–3788.

Sessions, A.L., and Hayes, J.M. (2005) Calculation of hydrogen isotopic fractionations in biogeochemical systems. *Geochim Cosmochim Acta* **69**: 593–597.

Sessions, A.L., Jahnke, L.L., Schimmelmann, A., and Hayes, J.M. (2002) Hydrogen isotope fractionation in lipids of the methane-oxidizing bacterium *Methylococcus capsulatus*. *Geochim Cosmochim Acta* **66**: 3955–3969.

Spaans, S., Weusthuis, R., Van Der Oost, J., and Kengen, S. (2015) NADPH-generating systems in bacteria and archaea. *Front Microbiol* **6**: 742.

Taubert, M., Stöckel, S., Geesink, P., Girnus, S., Jehmlich, N., von Bergen, M., *et al*. (2018) Tracking active groundwater microbes with D_2O labelling to understand their ecosystem function. *Environ Microbiol* **20**: 369–384.

Thauer, R.K. (1998) Biochemistry of methanogenesis: a tribute to Marjory Stephenson:1998 Marjory Stephenson prize lecture. *Microbiology* **144**: 2377–2406.

Thauer, R.K., Kaster, A.-K., Seedorf, H., Buckel, W., and Hedderich, R. (2008) Methanogenic archaea: ecologically relevant differences in energy conservation. *Nat Rev Microbiol* **6**: 579–591.

Valentine, D.L. (2009) Isotopic remembrance of metabolism past. *Proc Natl Acad Sci U S A* **106**: 12565–12566.

Valentine, D.L., Chidthaisong, A., Rice, A., Reeburgh, W.S., and Tyler, S.C. (2004b) Carbon and hydrogen isotope fractionation by moderately thermophilic methanogens. *Geochim Cosmochim Acta* **68**: 1571–1590.

Valentine, D.L., Sessions, A.L., Tyler, S.C., and Chidthaisong, A. (2004a) Hydrogen isotope fractionation during H_2/CO_2 acetogenesis: hydrogen utilization efficiency and the origin of lipid-bound hydrogen. *Geobiology* **2**: 179–188.

van der Meer, M.T.J., Benthien, A., French, K.L., Epping, E., Zondervan, I., Reichart, G.-J., *et al*. (2015) Large effect of irradiance on hydrogen isotope fractionation of alkenones in *Emiliania huxleyi*. *Geochim Cosmochim Acta* **160**: 16–24.

Vinokur, J.M., Cummins, M.C., Korman, T.P., and Bowie, J. U. (2016) An adaptation to life in acid through a novel mevalonate pathway. *Sci Rep* **6**: 39737.

Wang Y., Sessions A.L., Nielsen R.J., Goddard W.A (2013). Equilibrium 2H/1H fractionation in organic molecules: III. Cyclic ketones and hydrocarbons. *Geochimica et Cosmochimica Acta*, **107**: 82–95. http://dx.doi.org/10.1016/j.gca.2013.01.001.

Wegener, G., Bausch, M., Holler, T., Nguyen Manh, T., Mollar, X.P., Kellermann, M.Y., *et al*. (2012) Assessing sub-seafloor microbial activity by combined stable isotope probing with deuterated water and ^{13}C-bicarbonate. *Environ Microbiol* **14**: 1517–1527.

Wegener, G., Kellermann, M.Y., and Elvert, M. (2016) Tracking activity and function of microorganisms by stable isotope probing of membrane lipids. *Curr Opin Biotechnol* **41**: 43–52.

Weimer, P.J., and Zeikus, J.G. (1978) Acetate metabolism in *Methanosarcina barkeri*. *Arch Microbiol* **119**: 175–182.

Wijker, R.S., Sessions, A.L., Fuhrer, T., and Phan, M. (2019) ^{2}H/^{1}H variation in microbial lipids is controlled by NADPH metabolism. *Proc Natl Acad Sci U S A* **116**: 12173–12182.

Yin, X., Wu, W., Maeke, M., Richter-Heitmann, T., Kulkarni, A.C., Oni, O.E., *et al*. (2019) CO_2 conversion to methane and biomass in obligate methylotrophic methanogens in marine sediments. *ISME J* **13**: 2107–2119.

Yu, T., Wu, W., Liang, W., Lever, M.A., Hinrichs, K.-U., and Wang, F. (2018) Growth of sedimentary *Bathyarchaeotaon* lignin as an energy source. *Proc Natl Acad Sci U S A* **115**: 6022–6027.

Zehnder, A.J., and Brock, T.D. (1979) Methane formation and methane oxidation by methanogenic bacteria. *J Bacteriol* **137**: 420–432.

Zhang, X., Gillespie, A.L., and Sessions, A.L. (2009a) Large D/H variations in bacterial lipids reflect central metabolic pathways. *Proc Natl Acad Sci U S A* **106**: 12580–12586.

Zhang, Z., and Sachs, J.P. (2007) Hydrogen isotope fractionation in freshwater algae: I. Variations among lipids and species. *Org Geochem* **38**: 582–608.

Zhang, Z., Sachs, J.P., and Marchetti, A. (2009b) Hydrogen isotope fractionation in freshwater and marine algae: II. Temperature and nitrogen limited growth rate effects. *Org Geochem* **40**: 428–439.

Zhuang, G.-C., Elling, F.J., Nigro, L.M., Samarkin, V., Joye, S.B., Teske, A., and Hinrichs, K.-U. (2016) Multiple evidence for methylotrophic methanogenesis as the dominant methanogenic pathway in hypersaline sediments from the Orca Basin, Gulf of Mexico. *Geochim Cosmochim Acta* **187**: 1–20.

Supporting Information

Additional Supporting Information may be found in the online version of this article at the publisher's web-site:

Appendix 1. Supplementary experimental procedures.

Appendix 2. Supplementary figures and tables.

Fig. S1. Diether lipid biosynthetic pathway emphasizing carbon and hydrogen sources (Jain *et al*., 2014; Rodriguez and Leyh, 2014; Vinokur *et al*., 2016). Acetoacetyl-CoA tautomerizes and exchanges hydrogen with intercellular water, resulting in the hydrogen isotopic modification (Rodriguez and Leyh, 2014; Wang *et al*., 2013). Green, brown, and black H atoms are from water, NADPH and acetyl-CoA respectively. Bold hydrogen atoms refer to the possibility of isotopic exchange with water via tautomerization (Rodriguez and Leyh, 2014). The hydrogen atoms in the glycerol moiety labelled with question marks (?) may be from NADPH (Koga and Morii, 2007).

Fig. S2. Calibration curve of acetate and methanol standards on LC-IRMS. The x axis refers to carbon amount of acetate or methanol, the molar concentration (μM) of acetate and methanol was converted according to the carbon ratio of acetate and methanol of 0.40 and 0.374 respectively.

Fig. S3. Calibration curve of expected δD of water amended with different D_2O and measured δD.

Fig. S4. Hydrogen isotope ratio (R(D/H)) between NADPH and water for growth on acetate and methanol.

Table S1. δ^{13}C values of methane and acetate at time of harvest, and δ^{13}C and δD values of lipids produced by *M. barkeri* during the growth on labelled substrates (ca. 0.5%) and deuterated water (D_2O, 1%, 0.5% and 0.2%). n.d. = not detected. n.a. = not analysed.

Table S2. The Carbon isotope fractionation factor of lipid produced by *M. barkeri* grown on non-labelled H_2/CO_2, acetate and methanol. n.d., not detected. n.r., not reported.

Table S3. The hydrogen isotope fractionation factor between lipids and water produced by *M. barkeri* when grown on different substrates in natural water medium (δD = −50.6‰; red dash line). n.d., not detected.

Table S4. The mix ratio (%) of methane in headspace during incubation. The acceleration (***r***, % d^{-1}) of methane

accumulation in headspace was calculated during periods of linear increases (black values) in individual incubations via the linear regression. This rate was converted to methane production rate (r_2, μmol d^{-1}; Table S5) based on the ideal gas equation with headspace of 150 ml, constant pressure of 1 bar and temperature (308.15 K). The grey text indicates values that were not within the range of linear increase of methane and were excluded from rate calculations (cf. Penger *et al*., 2014).

Table S5. Summary of methane production rate (r_2), Gibbs energy, power supply conditions and water hydrogen assimilation factor (a_w).

Table S6. The labeling strategy for the incubation of *M*. *barkeri* on different substrates.

Text S1. Calculation of hydrogen isotopic composition of NADPH based isotopic mass balance.

Text S2. Gibbs free energy calculation under different conditions.